

## Article

# Binding Affinities Controlled by Shifting Conformational Equilibria: Opportunities and Limitations

Servaas Michielssens,<sup>1,2,\*</sup> Bert L. de Groot,<sup>1,\*</sup> and Helmut Grubmüller<sup>1,\*</sup><sup>1</sup>Department of Theoretical and Computational Biophysics, Max Planck Institute for Biophysical Chemistry, Göttingen, Germany; and<sup>2</sup>Department of Chemistry, Katholieke Universiteit Leuven, Leuven, Belgium

**ABSTRACT** Conformational selection is an established mechanism in molecular recognition. Despite its power to explain binding events, it is hardly used in protein/ligand design to modulate molecular recognition. Here, we explore the opportunities and limitations of design by conformational selection. Using appropriate thermodynamic cycles, our approach predicts the effects of a conformational shift on binding affinity and also allows one to disentangle the effects induced by a conformational shift from other effects influencing the binding affinity. The method is assessed and applied to explain the contribution of a conformational shift on the binding affinity of six ubiquitin mutants showing different conformational shifts in six different complexes.

## INTRODUCTION

Conformational plasticity is indispensable for the function of biomolecules. Conformational diversity allows a single molecular machine to perform multiple functions, react flexibly to signals (e.g., allosteric regulations), and permit promiscuous molecular recognition (1–4). Conformational plasticity is also most relevant for molecular evolution: substates with minor populations might explore new functionalities, whereas the main function remains intact (5). It is clear that distortions in or manipulations of the subtle conformational equilibria in biomolecular machines will alter their functionality, e.g., ligand-binding affinity or enzymatic catalysis. The populations of the substates can be modulated by posttranslational modifications, changes in environment, by mutations, or by binding of a second ligand. If delocalized conformational changes are involved, these modifications may be distant from the binding or active site, in which case the induced conformational shift gives rise to allostery.

One of the most prominent roles for conformational plasticity is in molecular recognition. The view is emerging that conformational selection (6–9) plays a role in most binding events. Because controlling molecular recognition is one of the major challenges in the field of biophysical chemistry (e.g., drug design, therapeutic proteins, understanding of biological pathways), the question naturally arises if—and to what extent—conformational selection can be exploited for that purpose.

To that end, three strategies to control molecular recognition can be distinguished. The first and most straightforward

strategy is to optimize direct interactions between the protein and its binding partner, e.g., by introducing hydrogen bonds, stacking interactions, etc. This strategy has been successfully applied for the design of small molecules (10–12) and in the design of proteins (13–15).

A second strategy is to reduce the loss of conformational entropy upon binding by rigidifying binding partners. This approach is well established in drug design (16) and has also been used in protein-protein recognition (17), e.g., via introduction of disulfide bonds (18).

The concept of conformational selection suggests a third strategy (19,20), outlined in Fig. 1 A. In this scenario, a biomolecule in equilibrium can adopt different structural conformations or substates, some of which are competent to bind to a specific binding partner whereas others are not. This property should enable control of both binding and selectivity by stabilizing or destabilizing different substates relative to the native biomolecule. Indeed, several examples have been reported where the effect of mutants was attributed to a change in the population of the binding-competent substate of the equilibrium ensemble (21–23). Although the concept of conformational preferences in the computation of free energies is well established (20,24,25), we here provide a general picture describing the effects of steering conformational preferences on binding affinities in a conformational selection scenario.

Particularly, we will explore and quantify opportunities and limitations in such a conformational selection-based approach. To that aim, we will use a suitable thermodynamic cycle (26) to predict how much the binding free energy will change due to an introduced conformational shift in different typical cases. Vice versa, this approach should enable one to calculate what fraction of an observed binding free-energy change can be attributed to a change in substate populations, and thus to separate

Submitted November 20, 2014, and accepted for publication April 15, 2015.

\*Correspondence: [servaas.michielssens@gmail.com](mailto:servaas.michielssens@gmail.com) or [bgroot@gwdg.de](mailto:bgroot@gwdg.de) or [hgrubmu@gwdg.de](mailto:hgrubmu@gwdg.de)

This is an open access article under the CC BY-NC-ND license (<http://creativecommons.org/licenses/by-nc-nd/4.0/>).

Editor: Michael Feig.

© 2015 The Authors

0006-3495/15/05/2585/6 \$2.00



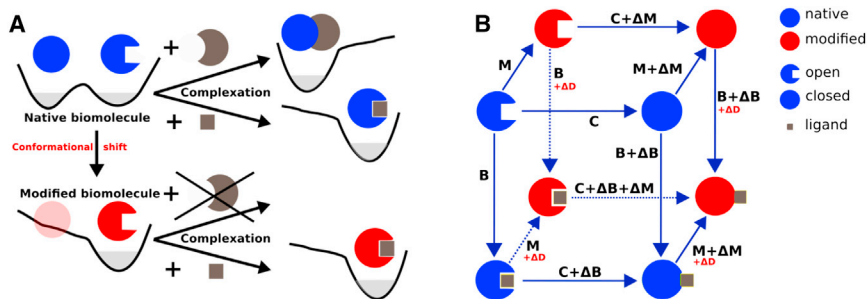


**FIGURE 1** (A) Conformational selection-based protein design. The native state of the protein has an open and a closed conformational state (blue, upper left), which are equally populated (light gray shades). These can be selected by different binding partners (dark gray). By modulating the populations of the different states (denoted by the color intensity of the symbols) and the underlying free-energy landscape) via mutations, selective binding can be achieved. (B) Thermodynamic cycle connecting the eight different states relevant for conformational selection-controlled binding. For explanation, see text. To see this figure in color, go online.

this effect from other, more direct effects such as enthalpic interactions.

To assess the potential of conformational selection-controlled molecular recognition, and to evaluate the accuracy and predictive value of our approach, we will use a comprehensive set of recently characterized mutations that induce conformational shifts in ubiquitin (27). Ubiquitin is an important signaling protein binding to a large set of quite diverse receptors. The dominant recognition mechanism is conformational selection, and the global dynamics of unbound ubiquitin captures all bound ubiquitin structures (4). This dynamics is largely described by a single collective motion, called the “pincer mode”, between an open and closed substate of ubiquitin. In most of the ubiquitin complexes, the binding partner prefers binding in either the open or the closed state (28), such that it should be possible to change the binding affinity via conformational shifts, which renders ubiquitin an excellent test system. To that end, a set of calculated binding free energies of six ubiquitin mutants with a known conformational shift to six different binding partners (27) will be considered.

## MATERIALS AND METHODS

### Conformational selection-controlled binding

To define notation and to derive an expression for the binding free-energy change  $\Delta\Delta G$  due to a conformational shift, we consider the thermodynamic cycle (or cube, in this case) in Fig. 1 B. This cycle describes a protein that binds to a ligand and occurs in two variants, denoted in Fig. 1 as native (blue) and modified (red). The modification can be a mutation, a posttranslational modification, allosteric changes, or any other effect. Each variant, in turn, is assumed to adopt two different conformations, here denoted by the terms “open” and “closed”.

By definition,  $\Delta\Delta G$  is the difference between the ligand binding free energies  $\Delta G$  of the modified protein and that of the native one, which reads in terms of the respective partition functions  $Z$ ,

$$\Delta\Delta G = \Delta G^{\text{modified}} - \Delta G^{\text{native}} = -\frac{1}{\beta} \ln \frac{Z_{\text{bound}}^{\text{modified}} Z_{\text{unbound}}^{\text{native}}}{Z_{\text{unbound}}^{\text{modified}} Z_{\text{bound}}^{\text{native}}}. \quad (1)$$

Here,  $\beta$  is the reciprocal thermal energy  $k_B T$ . To obtain an easily interpretable expression for  $\Delta\Delta G$ , the following relevant free-energy differences

are considered (see also Fig. 1 B):  $B$  is the binding affinity of the open native state;  $C$  is the conformational free-energy difference between open and closed unbound states, which defines the relative populations of their conformational equilibrium;  $M$  is the free-energy change of the open unbound state due to the modification;  $\Delta B$  is the difference between the binding free energy of the closed native state and that of the open native state; and  $\Delta M$  is the change of the conformational free-energy difference  $C$  due to the conformational shift induced by the protein modification.

Note that, via the closure relation for the unbound states (upper-half of Fig. 1 B),  $\Delta M$  also denotes the difference between the free-energy change  $M$  of the open unbound state due to the modification and that of the closed unbound state.

Other than shifting conformational equilibria, the modification can also modify the binding affinity more directly, e.g., by local interactions. Such effects will be collected in the term  $\Delta D$  and considered separately further below.

With this notation, all free-energy differences marked by arrows are readily expressed as indicated in Fig. 1 B in such a way that the respective closure relations are fulfilled, i.e., the sum over all closed paths is zero. These expressions, in turn, allow us to expand all four partition functions above, each of which is composed of two conformational substates:

$$\begin{aligned} Z_{\text{unbound}}^{\text{native}} &= e^0 + e^{-\beta C}, \\ Z_{\text{bound}}^{\text{native}} &= e^{-\beta B} + e^{-\beta(B+C+\Delta B)}, \\ Z_{\text{unbound}}^{\text{modified}} &= e^{-\beta M} + e^{-\beta(M+C+\Delta M)}, \\ Z_{\text{bound}}^{\text{modified}} &= e^{-\beta(M+B+\Delta D)} + e^{-\beta(M+B+\Delta D+C+\Delta B+\Delta M)}. \end{aligned}$$

Note that, without loss of generality, the absolute free energy of the native open unbound state was set to zero.

With these four partition functions, the binding free-energy change  $\Delta\Delta G$  reads

$$\Delta\Delta G = \Delta D - \frac{1}{\beta} \ln \frac{(1 + e^{-\beta(C+\Delta B+\Delta M)})(1 + e^{-\beta C})}{(1 + e^{-\beta(C+\Delta M)})(1 + e^{-\beta(C+\Delta B)})}. \quad (2)$$

Notably, this expression is independent of the free-energy difference  $M$  between native and modified protein, which canceled out. As should be expected,  $\Delta\Delta G$  is composed of the direct effect of the modification of binding affinity,  $\Delta D$ , and a contribution due to the conformational shift free energy,  $\Delta M$ . We will subsequently focus on the latter, but note that this fact allows one to separate  $\Delta D$  from a set of determined affinities by comparing the (measured or calculated) total change in free energy with the right-hand term in Eq. 2. The remaining two relevant parameters are thus the free-energy difference  $C$  between native open and closed substates, and their differential binding affinity  $\Delta B$ .

## Simulations and calculations

Six different ubiquitin complexes studied in Michielsens et al. (27) were considered; their structures were taken from the Protein Data Bank (PDB) (29). Three of these complexes bind ubiquitin in the open substate (Ubiquitin Carboxyl-terminal esterase L3 (UCH-L3, PDB:1XD3), Rab5 GDP/GTP exchange factor (PDB:2FIF), and the UBA domain of Dsk2 (PDB:4UN2),  $\Delta B > 0$ ). Two of them bind ubiquitin in the closed substate (UBA domain of Dsk2 (PDB:1NBF) and Ubiquitin carboxyl-terminal hydrolase 5 (PDB:2G45),  $\Delta B < 0$ ). One has no preference for either of the states (vacuolar protein sorting protein 36 (PDB:2HTH),  $\Delta B \approx 0$ ).

For each of these six complexes, binding free-energy changes  $\Delta\Delta G$  for all six mutants were taken from previously determined binding free energies (27). Free-energy differences  $\Delta M$  and  $C$  for these six mutations were taken from previous alchemical calculations (27).

Neither experimental nor calculated binding affinity differences between the open and closed native state were available; these were, therefore, calculated here from additional umbrella sampling molecular dynamics (MD) simulations of free ubiquitin and of ubiquitin in the six different complexes.  $\Delta B$  was then determined from the difference between the free ubiquitin conformational free-energy difference  $C$  (see Fig. 1 B) and that of the respective complex,  $C + \Delta B$ .

All simulations were set up and carried out as described previously (27). For the umbrella sampling, the pincer mode (collective mode describing the open-closing motion) identified previously (4) was used as a reaction coordinate. Twenty-one umbrella windows were used. The minima of the windows were placed at equidistant positions along this collective coordinate between  $-1.0$  and  $0.5$  nm. The initial structure for each umbrella simulation was selected as the structure closest to the respective umbrella potential minimum from a free MD simulation of the complex. Note that in three of the complexes (PDB:1XD3, PDB:1NBF, and PDB:2FIF), ubiquitin explores only either the open or the closed state. In those cases the essential dynamics module of GROMACS (30,31) using fixed step linear expansion was used to generate starting structures for the umbrella sampling simulations (32,33). A force constant of  $1000$  kJ/(mol nm<sup>2</sup>) was applied, using the pincer mode as a reaction coordinate. For each of the umbrella windows, 10 simulations of 120 ns each were performed, each starting from different velocities chosen from a Maxwell distribution. To eliminate initial relaxation effects, only the last 100 ns of each simulation were used for subsequent analysis. The total simulation time for umbrella sampling simulations was  $25.2$   $\mu$ s. The free-energy profile was determined using WHAM (34), and the error was estimated using Bayesian bootstrapping of complete histograms as implemented in G\_WHAM (35).

Using the above free-energy differences, the expected contributions of conformational selection to the binding free-energy changes were calculated from Eq. 2.

## RESULTS AND DISCUSSION

### Conformational selection-controlled binding

Fig. 2 illustrates the effect of  $C$  and  $\Delta B$  on  $\Delta\Delta G$  as a function of conformational shift free-energy  $\Delta M$ . We will restrict our discussion to the upper part of Fig. 2 ( $C \leq 0$ ); the lower part ( $C < 0$ ) is related by symmetry and is shown to provide the full picture and serves as an orientation for the reader.

For  $C \leq 0$ , four scenarios can be distinguished: First, if the binding-competent state forms a major population (*red-dish curves*), the potential to improve the binding affinity is limited. However, a significant destabilization of the complex can be achieved by relative stabilization of the bind-

ing-incompetent state, by maximally  $|C| + |\Delta B|$ . Second, in contrast, if the binding-competent state forms a minor population (*blue and green curves*), significant affinity gains by up to maximum ( $|\Delta B|, |C|$ ) can be reached by relative stabilization of the binding-competent state. As a typical case, consider, e.g., a dominant open state with preferred binding to the closed state. In this case, already a shift of 10 kJ/mol (*blue curves*) changes the binding affinity from the micromolar to the nanomolar range. Destabilization of up to maximum ( $|\Delta B| - |C|, 0$ ) can be achieved by a conformational shift toward the binding-incompetent conformation. This limit is reached if  $|\Delta M|$  and  $|C|$  compensate for  $|\Delta B|$ . If, third, the binding-competent and incompetent states have similar populations, no large gain in binding affinity is expected. Rather, more selective binding can be achieved by a conformational shift that exclusively populates one of the conformations. Fourth, if both states have similar affinities, no affinity or selectivity change can be induced by a conformational shift. Hence,  $\Delta B \neq 0$  is a necessary condition for a conformational shift strategy to affect binding affinity.

### Application to ubiquitin binding

Six mutations in ubiquitin were considered (Fig. 3), the conformational free-energy shifts  $\Delta M$  (*dashed lines*, see also Fig. 1 B) of which have been previously calculated from MD simulations (27). As can be seen, two of the mutations shift the conformational equilibrium of the unbound state toward the closed state (L69S, L69T,  $\Delta M < 0$ ), two others toward the open state (I13F, I36A,  $\Delta M > 0$ ), and the remaining two do not largely affect the conformational equilibrium (V5L, I36L,  $\Delta M \approx 0$ ).

The colored lines in Fig. 3 quantify the expected binding free-energy changes  $\Delta\Delta G$  according to Eq. 2 for each of the six ubiquitin complexes as a function of the conformational free-energy shift  $\Delta M$ . The respective intersections with the dashed lines, therefore, denote the binding free-energy changes for each of the mutations, as predicted by our conformational selection framework. Because the free-energy difference  $C$  between the open and closed states of free ubiquitin is only 1.7 kJ/mol, both the open and the closed state are expected to be similarly populated. Accordingly, the third case of small  $C$  considered above applies, for which the binding-competent state is already relatively abundant for both the open- and closed-state-preferring binding partners. Therefore, the potential to increase the binding strength is limited.

These six predicted binding free-energy changes are compared in Fig. 4 to those calculated previously from alchemical calculations. Because the former only describe the contribution of conformational selection to the total binding free energies, no full agreement (*black diagonal*) is expected; nevertheless, over the entire dataset an average unsigned deviation of only 3.85 kJ/mol is obtained.

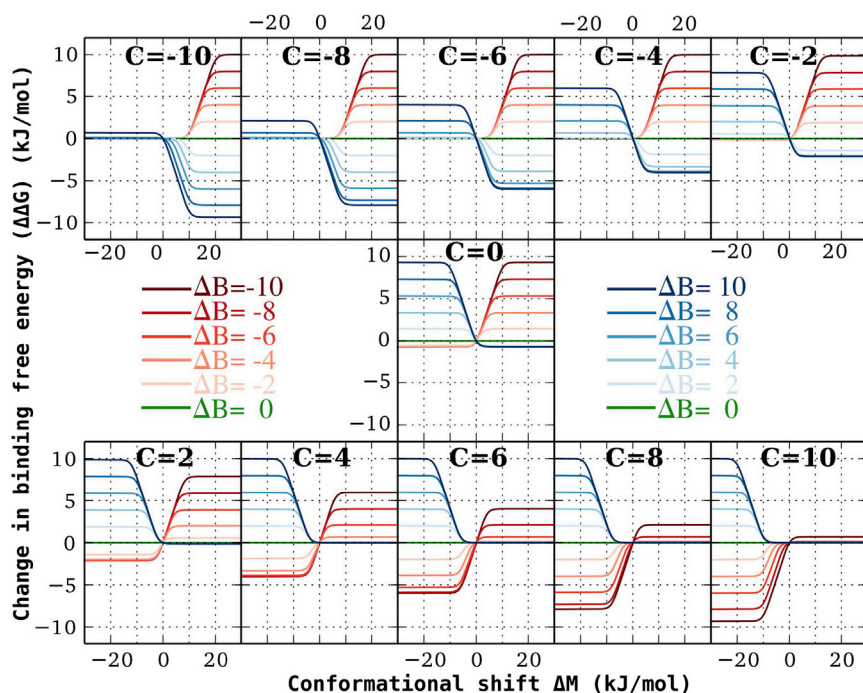


FIGURE 2 Various scenarios for the effect of a conformational shift by mutation on the binding affinity  $\Delta\Delta G$  as discussed in the text. The plots differ by the population of the native state equilibria (described by  $C$ ). In each plot, the different curves (colors) describe binding preference  $\Delta B$  to the open ( $\Delta B > 0$ ) or closed ( $\Delta B < 0$ ) state. To see this figure in color, go online.

Remarkably, the predicted values correlate well with the calculated data with a correlation coefficient of 0.56 ( $N = 36$ ).

On average, the binding free-energy changes predicted from a pure conformational selection scenario (black diagonal in Fig. 4) are smaller than the calculated ones by a factor of five (blue linear fit). To assess the significance of this deviation, we considered two factors.

The first factor is that there is a statistical uncertainty in both the direct calculation of  $\Delta\Delta G$  and the calculation of  $\Delta\Delta G$  via the conformational shift. Considering the resulting

error bars (obtained by bootstrapping, see the Supporting Material), 75% of all mutations in all complexes are within 2 SDs from the binding affinities expected from the conformational shifts alone. If this were the only effect, and assuming a Gaussian error distribution, one would expect 95% of all results to fall within this interval. This indicates that the statistical uncertainty alone is not sufficient to explain the observed differences. Additionally, we expect that, due to insufficient sampling, our alchemical calculations tend to overestimate the mutation-induced destabilization of protein-protein complexes in those cases where the

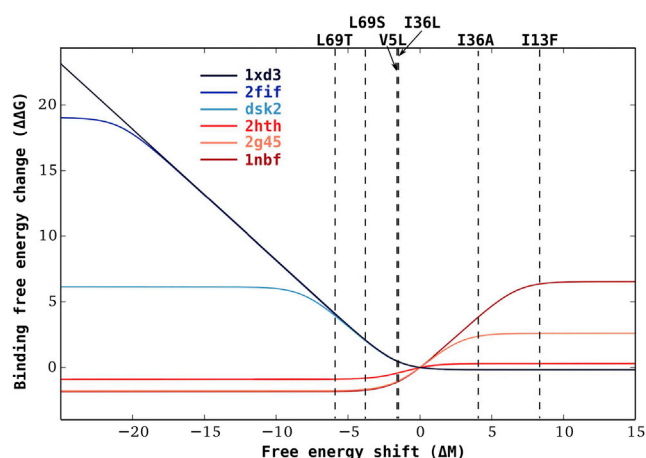


FIGURE 3 Predicted binding free-energy changes  $\Delta\Delta G$  (colored lines) due to six different ubiquitin mutants in six different complexes. (Dashed lines) Calculated conformational free-energy shifts  $\Delta M$  for six point mutants (27). To see this figure in color, go online.

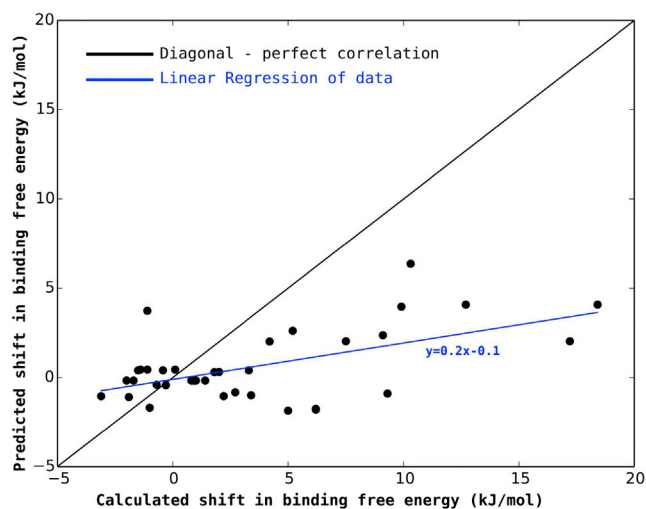


FIGURE 4 Comparison between predicted and calculated binding free-energy changes. (Black solid line) Perfect agreement; (blue line) linear regression fit. To see this figure in color, go online.

free-energy minimum of the mutant is separated from that of the native state by a slow structural transition. The L69T ubiquitin mutant in complex with the *dsk2* protein is one such example, where it was found that the experimental destabilization due to the mutation was markedly lower than the calculated value (27).

The second factor suggests an interesting application of our analysis, namely that additional effects can be quantified via their effect on  $\Delta\Delta G$ . If all required parameters as well as the observed effect on  $\Delta\Delta G$  are at hand, Eq. 2 can be used to separate the effect caused by a conformational shift from other factors via  $\Delta D$ . Although the mutations were intentionally introduced in the hydrophobic core of ubiquitin to minimize direct effects on  $\Delta\Delta G$ , these cannot be fully ruled out. If this analysis were correct, and because  $\Delta D$  enters into Eq. 2 only as an offset, any direct effects should decrease with increasing distance of the mutation site from the binding interface.

This idea is tested in Fig. 5, which shows  $\Delta D$ , estimated from the differences between predicted and calculated free-energy shifts  $\Delta\Delta G$ , as a function of the distance of the respective mutation from the binding site (also listed in Fig. 5). Indeed, the estimated  $\Delta D$  values systematically decrease with increasing distance. The largest  $|\Delta D|$  values are seen for mutations close to the binding interface (3.38–6.75 Å) (L69S-1NBF, L69T-1NBF, L69T-2G45, I36L-1XD3, and L69T-2HTH), where only a small effect is predicted but significant destabilization ( $>1$  kcal/mol) is observed. Also, the mutation I36A-1NBF should destabilize the complex, but no significant effect is observed. In contrast, for mutations where the distance is larger than 8 Å (15 mutations), an average unsigned error of 1.5 kJ/mol and a correlation coefficient of 0.72 is obtained. Notably, for the distant mutations, 87% of the

predicted binding free-energy changes fall within the 95% confidence interval, corroborating that these deviations can be largely explained by the statistical uncertainty of the free-energy calculations. For these cases, therefore, direct effects seem to be small.

For free ubiquitin, the free-energy difference  $C$  between the open and closed states was found to be small and hence, the potential for enhancing affinities is small, in agreement with the binding free energies found in the six mutations in the six complexes. For other cases, where the binding-competent state is sparsely populated, larger affinity gains are expected. Further, according to our analysis, a substantial increase of binding selectivity for ubiquitin should be possible by reducing the binding strength, thus shifting the equilibrium toward the binding-incompatible conformation. This direct connection between conformational selection-controlled affinity and selectivity is a feature that may be useful for pharmacological applications.

We have developed a quantitative method to predict the effect of a mutation-induced conformational shift on binding affinity via conformational selection. This method can serve to guide an emerging protein design strategy where protein-protein binding is optimized using conformational shifts. Within this framework, binding affinity changes are predicted quantitatively if substate populations in the wild-type, and preference for a given substate of the binding partner, are known. The framework can further be used to determine what fraction of the change in binding free energy ( $\Delta\Delta G$ ) is due to conformational shift, and thus can be disentangled from other, direct binding interactions.

The method was tested against a dataset of six ubiquitin mutants with known conformational shifts and known preferences for the involved conformational substates. The observed effects were found to agree well with our predictions.

This work characterizes the opportunities and limitations of modulating conformational equilibria to control biomolecular properties. Although the focus here was mainly on exploring the effect due to mutations, our method is quite general and thus serves to rationalize the effects of conformational modulations on allosteric regulation, posttranslational modifications, or environmental changes.

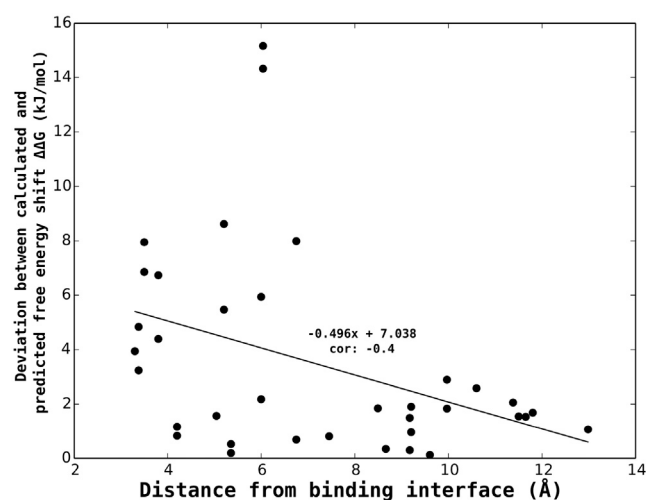


FIGURE 5 Deviation (symbols) between predicted binding free-energy changes (based on the conformational shift) and calculated changes from alchemical mutational free-energy changes in complexes (27) as a function of the distance from the binding interface. (Solid line) Linear regression fit.

## SUPPORTING MATERIAL

One table is available at [http://www.biophysj.org/biophysj/S0006-3495\(15\)00390-2](http://www.biophysj.org/biophysj/S0006-3495(15)00390-2).

## AUTHOR CONTRIBUTIONS

S.M., B.L.d.G., and H.G. designed research; S.M. performed research; S.M., B.L.d.G., and H.G. analyzed data; and S.M., B.L.d.G., and H.G. wrote the article.

## REFERENCES

- James, L. C., and D. S. Tawfik. 2003. Conformational diversity and protein evolution—a 60-year-old hypothesis revisited. *Trends Biochem. Sci.* 28:361–368.
- James, L. C., P. Roversi, and D. S. Tawfik. 2003. Antibody multispecificity mediated by conformational diversity. *Science*. 299:1362–1367.
- Lefstin, J. A., and K. R. Yamamoto. 1998. Allosteric effects of DNA on transcriptional regulators. *Nature*. 392:885–888.
- Lange, O. F., N. A. Lakomek, ..., B. L. de Groot. 2008. Recognition dynamics up to microseconds revealed from an RDC-derived ubiquitin ensemble in solution. *Science*. 320:1471–1475.
- Tokuriki, N., and D. S. Tawfik. 2009. Protein dynamism and evolvability. *Science*. 324:203–207.
- Boehr, D. D., R. Nussinov, and P. E. Wright. 2009. The role of dynamic conformational ensembles in biomolecular recognition. *Nat. Chem. Biol.* 5:789–796.
- Changeux, J.-P., and S. Edelstein. 2011. Conformational selection or induced fit? 50 years of debate resolved. *F1000 Biol. Rep.* 3:19.
- Ma, B., S. Kumar, ..., R. Nussinov. 1999. Folding funnels and binding mechanisms. *Protein Eng.* 12:713–720.
- Tsai, C. J., B. Ma, and R. Nussinov. 1999. Folding and binding cascades: shifts in energy landscapes. *Proc. Natl. Acad. Sci. USA*. 96:9970–9972.
- Cui, J. J., M. Tran-Dubé, ..., M. P. Edwards. 2011. Structure-based drug design of crizotinib (PF-02341066), a potent and selective dual inhibitor of mesenchymal-epithelial transition factor (c-MET) kinase and anaplastic lymphoma kinase (ALK). *J. Med. Chem.* 54:6342–6363.
- Congreve, M., S. P. Andrews, ..., F. H. Marshall. 2012. Discovery of 1,2,4-triazine derivatives as adenosine A(2A) antagonists using structure based drug design. *J. Med. Chem.* 55:1898–1903.
- Seeliger, D., C. Zapater, ..., B. L. de Groot. 2013. Discovery of novel human aquaporin-1 blockers. *ACS Chem. Biol.* 8:249–256.
- Fleishman, S. J., T. A. Whitehead, ..., D. Baker. 2011. Computational design of proteins targeting the conserved stem region of influenza hemagglutinin. *Science*. 332:816–821.
- Karanicolas, J., J. E. Corn, ..., D. Baker. 2011. A de novo protein binding pair by computational design and directed evolution. *Mol. Cell*. 42:250–260.
- Whitehead, T. A., D. Baker, and S. J. Fleishman. 2013. Computational design of novel protein binders and experimental affinity maturation. *Methods Enzymol.* 523:1–19.
- Kitchen, D. B., H. Decornez, ..., J. Bajorath. 2004. Docking and scoring in virtual screening for drug discovery: methods and applications. *Nat. Rev. Drug Discov.* 3:935–949.
- Kamisetty, H., A. Ramanathan, ..., C. J. Langmead. 2011. Accounting for conformational entropy in predicting binding free energies of protein-protein interactions. *Proteins*. 79:444–462.
- Zhang, Y., L. Zhou, ..., J. E. Corn. 2013. Conformational stabilization of ubiquitin yields potent and selective inhibitors of USP7. *Nat. Chem. Biol.* 9:51–58.
- Hauryliuk, V., S. Hansson, and M. Ehrenberg. 2008. Cofactor dependent conformational switching of GTPases. *Biophys. J.* 95:1704–1715.
- Aleksandrov, A., D. Thompson, and T. Simonson. 2010. Alchemical free energy simulations for biological complexes: powerful but temperamental. *J. Mol. Recognit.* 23:117–127.
- Bouvignies, G., P. Vallurupalli, ..., L. E. Kay. 2011. Solution structure of a minor and transiently formed state of a T4 lysozyme mutant. *Nature*. 477:111–114.
- Ådén, J., A. Verma, ..., M. Wolf-Watz. 2012. Modulation of a pre-existing conformational equilibrium tunes adenylate kinase activity. *J. Am. Chem. Soc.* 134:16562–16570.
- Haririnia, A., R. Verma, ..., D. Fushman. 2008. Mutations in the hydrophobic core of ubiquitin differentially affect its recognition by receptor proteins. *J. Mol. Biol.* 375:979–996.
- Mobley, D. L., J. D. Chodera, and K. A. Dill. 2007. The confine-and-release method: obtaining correct binding free energies in the presence of protein conformational change. *J. Chem. Theory Comput.* 3:1231–1235.
- Galicchio, E., and R. M. Levy. 2011. Recent theoretical and computational advances for modeling protein-ligand binding affinities. In *Computational Chemistry Methods in Structural Biology, Vol. 85* C. Christov, editor. Academic Press, New York.
- van Gunsteren, W. F., and H. J. Berendsen. 1987. Thermodynamic cycle integration by computer simulation as a tool for obtaining free energy differences in molecular chemistry. *J. Comput. Aided Mol. Des.* 1:171–176.
- Michielssens, S., J. H. Peters, ..., B. L. de Groot. 2014. A designed conformational shift to control protein binding specificity. *Angew. Chem.* 53:10367–10371.
- Peters, J. H., and B. L. de Groot. 2012. Ubiquitin dynamics in complexes reveal molecular recognition mechanisms beyond induced fit and conformational selection. *PLoS Comput. Biol.* 8:e1002704.
- Bernstein, F. C., T. F. Koetzle, ..., M. Tasumi. 1978. The Protein Data Bank: a computer-based archival file for macromolecular structures. *Arch. Biochem. Biophys.* 185:584–591.
- Hess, B., C. Kutzner, ..., E. Lindahl. 2008. GROMACS 4: algorithms for highly efficient, load-balanced, and scalable molecular simulation. *J. Chem. Theory Comput.* 4:435–447.
- van der Spoel, D., E. Lindahl, ..., H. J. C. Berendsen. 2010. GROMACS User Manual, Ver. 4.5.4. [www.gromacs.org](http://www.gromacs.org).
- Amadei, A., A. B. M. Linssen, ..., H. J. C. Berendsen. 1996. An efficient method for sampling the essential subspace of proteins. *J. Biomol. Struct. Dyn.* 13:615–625.
- de Groot, B. L., A. Amadei, ..., H. J. C. Berendsen. 1996. An extended sampling of the configurational space of HPr from *E. coli*. *Proteins*. 26:314–322.
- Kumar, S., J. M. Rosenberg, ..., P. A. Kollman. 1992. The weighted histogram analysis method for free-energy calculations on biomolecules. I. The method. *J. Comput. Chem.* 13:1011–1021.
- Hub, J. S., B. L. de Groot, and D. van der Spoel. 2010. G\_WHAM—a free weighted histogram analysis implementation including robust error and autocorrelation estimates. *JCTC*. 6:3713–3720.